Lawrence Berkeley National Laboratory
Recent Work

Title
Resolving magnetic and chemical correlations in CoPtCr films using soft X-ray resonant scattering

Permalink
https://escholarship.org/uc/item/80x83814

Journal
Journal of Magnetism and Magnetic Materials, 240(1/3/2008)

Authors
Kortright, J.B.
Hellwig, O.
Marguiles, D.T.
et al.

Publication Date
2001-07-27

Resolving magnetic and chemical correlations in CoPtCr films

using soft x-ray resonant scattering

J. B. Kortright,[a]* O. Hellwig,[b] D. T. Margulies,[b] and Eric E. Fullerton[b]

*a*Materials Sciences Division, Lawrence Berkeley National Laboratory, Berkeley, California, 94720, USA

*b*IBM Almaden Research Center, 650 Harry Road, San Jose, California, 95120, USA

Abstract

Resonant small-angle scattering at the $2p$ levels of $3d$ transition elements strongly enhances scattering from both magnetic and chemical structure in the plane of thin films, as recently demonstrated for Co/Pt multilayers having perpendicular anisotropy. Here this resonant enhancement is demonstrated for CoPtCr films having in-plane magnetic anisotropy. A simple formalism describing the spectral dependence of the kinematical scattering provides a means to distinguish between magnetic and charge scattering and to probe the chemical segregation processes yielding charge scattering, thereby providing new information about this structure. It is found that correlation lengths of magnetic scattering are roughly 5 times larger than those for chemical scattering in the as-deposited CoPtCr film studied, consistent with significant exchange-coupling between polycrystalline grains.

Keywords: magnetic recording media, magnetic structure, grain size, x-ray scattering, core levels

*Corresponding author, Tel.: 1-510-486-5960; fax: 1-510-486-5330.

E-mail address: JBKortright@lbl.gov

1. Introduction

Increasing technological importance of thin films involving single or multiple layers ranging from less than one to tens of nanometers thick calls for improved methods to understand the interrelationships between magnetic and chemical structure that determine magnetic interactions, energies, and transport properties of interest. Such thin films typically involve heterogeneity (*i.e.*, structure) both in magnetic and chemical (or compositional) properties. Understanding the spatial correlation of magnetic and chemical properties at the relevant length scales both perpendicular to and in the plane of the films is thus of great importance. Relevant length scales include characteristic magnetic lengths ranging from interatomic dimensions to domain sizes ≥ 100 nm, and also any length scales of chemical heterogeneity. Length scales of in-plane chemical heterogeneity (segregation, polycrystalline grain structure, surface or interface roughness, etc.) are often of the order of the film thickness. Thus techniques capable of simultaneously resolving both magnetic and chemical structure with resolution ranging from atomic to tens of nanometers are especially valuable.

Resonant spectroscopies at the $2p$ core levels of the magnetic $3d$ transition metals offer various signals that can provide insight into magnetic and chemical structure in films [1]. Soft x-ray wavelengths in this $1 - 2$ nm range set the spatial resolution limit of purely photon based techniques, and in many cases the utility of the strong, element-specific resonant signals outweighs the loss of sub-angstrom resolution typical in the hard x-ray spectral range. Its position between the hard x-ray and near-visible spectral regions suggests adoption of formalisms common in both x-ray and visible magnetooptical studies [2]. Soft x-ray Faraday (transmission) and Kerr (reflection) geometry measurements involve forward and specular scattered beams, respectively, and thus provide information averaging over in-plane magnetic and chemical structure. Even so, these techniques can provide depth-resolution with nm and sub-nm resolution in various ways: tuning to a core level of an ultrathin chemical marker layer is one approach [3]; another is to radically alter the skin depth by tuning across a strong L_3 white line [4]; and yet another uses strong interference from interfaces in multilayer films as a tunable depth probe across buried interfaces [5].

Diffuse resonant scattering techniques offer a means to gain sensitivity to *in-plane* magnetic and chemical structure. Diffuse scattering can be measured in reflection geometry away from the specular condition [6, 7, 8, 9], in which case the scattering vector **q** necessarily probes both out-of-plane and in-plane structure. Diffuse scattering in the transmission geometry probes in-plane structure more directly, and is used here. Compared to microscopy techniques, incoherent scattering techniques provide ensemble-averaged information about magnetic and chemical structure, albeit with quite good spatial resolution. Coherent resonant magnetic scattering techniques are under development that retain local structure information and offer potential for time-resolved information down to the nanosecond regime [10].

This paper extends a recent study of magnetic and chemical structure in Co/Pt multilayer films having perpendicular magnetic anisotropy [11] to single-layer films having in-plane magnetic anisotropy. Discussion of general and specific experimental considerations is followed by results and analysis for a CoPtCr film of interest for longitudinal magnetic recording. Emphasis is placed on the analysis of the spectral dependence of the scattering and its use to identify and begin to quantify sources of scattering. For the film studied we find magnetic correlation lengths roughly five times larger than chemical correlation lengths, consistent with significant exchange coupling between adjacent polycrystalline grains.

2. General considerations

The symmetric transmission small-angle scattering (SAS) geometry used here is shown in Figure 1. Measurements were made by scanning an aperture at scattering angle $2q$ and the sample at angle q to keep **q** (having magnitude $q = 4\pi \sin q / l$ for wavelength l) strictly in the film plane. Since $2q$ is small, measurement using a position-sensitive detector and sample fixed at normal incidence also maintains **q** predominantly in the film plane. In addition to optimizing the coupling to in-plane magnetic and chemical structure, this geometry has the advantage of a well-defined sample volume. In comparison, off-specular reflection geometry measurements of diffuse scattering couple less directly to in-plane

structure, and can suffer from varying penetration depth with energy and angle [2] and interference and distorted-wave effects [2, 12], all of which lead to variations in effective sample volume and hence measured intensities.

Linear incident polarization is appropriate for measuring diffuse magnetic (and chemical) scattering, since linear polarization is composed of a coherent superposition of + and − helicity circular components. These orthogonal modes do not mix in the scattering process, so that magnetic scattering using linear polarization is equivalent to scattering using circular polarization of each helicity simultaneously [11]. Thus we consider magnetic scattering of circular components below, realizing that the intensities of each circular component are added to give the total intensity for incident linear polarization.

Two limiting cases for magnetic domain structure in films are shown in Fig. 1. Figure 1a shows magnetic domains in a film having perpendicular anisotropy, as considered in ref. 11 for Co/Pt multilayers. In this geometry the full polarization dependence of the Co resonant magnetic scattering factor for circular components simplifies to $f_{+/-} \cong f_c \pm f_m$ where f_c is the resonant plus non-resonant charge scattering factor and f_m is the resonant dipole term first order in magnetization $\mathbf{M}$ describing the predominant magnetic scattering in ferromagnetic samples [2, 11]. Here the dipole term 2nd order in $\mathbf{M}$ and higher multipole transition terms are neglected. This is reasonable for resonant scattering at the $2p$ levels of $3d$ transition elements, although higher multipole terms are clearly important as l decreases. Perpendicular $\mathbf{M}$ and small $\boldsymbol{q}$ maximize sensitivity to f_m and hence to scattering from resonant magnetic structure in the plane of the film. Figure 1b depicts magnetic domains in films with in-plane anisotropy, as one would encounter in longitudinal recording, and is relevant to the CoPtCr film studied here. In this geometry the effective Co resonant magnetic scattering factor is $f_{+/-} \cong f_c \pm \sin(2\boldsymbol{q}) f_m$, and sensitivity to domains is reduced compared to the perpendicular anisotropy case. Even with this reduced magnetic sensitivity, the large resonant effects make it possible to observe magnetic SAS for films with in-plane structure in this geometry.

Diffuse SAS results from contrast in scattering amplitude between two or more different phases. Let us call a_i the scattering amplitude for phase i, realizing that it is given by some linear combination of scattering factors of the different species making up that phase. Then the total scattering amplitude for a heterogeneous film is $A = \sum_i a_i s_i$ with s_i the structure factor describing the spatial distribution of phase i. In the kinematical (single scattering) approximation the scattered intensity $I = A^* A$. Assuming two terms corresponding to magnetic and chemical scattering, this formalism predicts intensity terms corresponding to magnetic-magnetic and charge-charge correlations, as well as a term corresponding to charge-magnetic interference [11, 13]. The spectral dependence of the different intensity terms is determined primarily by the $a_i^* a_j$ at fixed q in this transmission SAS geometry, $i.e.$, by the spectral dependence of the resonant scattering factors together with any non-resonant scattering factors contributing to amplitude contrast. Below the measured spectral dependence of these factors is modeled using measured Co resonant magnetic (and charge) scattering factors.

3. Experimental details

The film studied here has nominal composition $Co_{69}Pt_9Cr_{22}$, is 32 nm thick, and was deposited by magnetron sputtering atop buffer layers that were grown onto a 160 nm thick SiN_x membrane for transmission measurements. A 5 nm carbon layer tops the structure. The polycrystalline CoPtCr layer has the c axis of the hcp crystal structure in-plane with random in-plane anisotropy, and closely simulates a generation of longitudinal recording media films in which some degree of chemical segregation to the polycrystalline grain boundaries is thought to limit intergrain exchange coupling and account for the recording properties [14, 15]. Determining the magnetic and chemical correlation lengths in an as-deposited film using resonant soft x-ray scattering is thus an initial goal of studies of this and related systems.

Measurements were made using two different beamlines at LBNL's Advanced Light Source. Diffuse scattering q and $h\boldsymbol{n}$ scans were measured on bending magnet beamline 6.3.2. using a broad vertical fan of

radiation and hence a range of polarization states (all of which can be described as superpositions of varying amounts of opposite helicity circular components). Diffuse scattering was also measured in the elliptically polarizing undulator beamline 4.0 using linear polarization. This beamline, tuned to have degree of circular polarization 0.9, was also used to measure the transmission absorption spectra across the Co $2p$ levels at a 45° incidence angle with $\mathbf{M}$ saturated in-plane and in the scattering plane. Comparison of absorption spectra of the alloy film with those from a thicker Co film suggests that thickness effects [2] at the Co L_3 line are not severe in these measurements. The absorption spectra where then normalized to $\mathrm{Im}[f_{+/-}]$ from which the dispersive part of $\mathrm{Re}[f_{+/-}]$ were obtained via Kramers-Krönig transformation, thus yielding the complete resonant charge and magnetic scattering factors for Co shown below. The real, non-dispersive charge term $f_o = Z$ must be added to obtain the complete charge scattering factor f_c [2, 11].

4. Results and Discussion

Radial scans through reciprocal space (q scans) at a series of fixed x-ray energies are shown in Fig. 2, and exhibit two separate peaks with distinctly different energy dependence. These data are normalized by the time variation of the incident intensity, but not by the strong energy dependence of the sample's transmission spectrum. The peak at lower $q \cong 0.013 \, \text{Å}^{-1}$ indicates scattering from interfering features separated by roughly $2\pi/q = 48$ nm. The peak at higher $q \cong 0.057 \, \text{Å}^{-1}$ corresponds to interfering features roughly 11 nm apart. The presence of two peaks indicates two distinct length scales in this sample. The shorter length scale is close to the average size of polycrystalline grains in these media films as determined by TEM [14]. In analogy with the two peaks observed in scattering from Co/Pt multilayers in ref. 11, it is natural to hypothesize that the longer length scale corresponds to a magnetic correlation length or domain spacing. Such a peak could result, for example, if the magnetization of several adjacent grains was strongly correlated to yield a magnetic length scale larger than the grain size. Up to now direct experimental measurements of magnetic correlation lengths in such films have not been possible.

Magnetic correlation lengths have been inferred from magnetic recording signal to noise measurements and have, in general, been found to be larger than the polycrystalline grain size [16].

The energy dependence of the scattering at the two peaks offers clear evidence that they originate predominantly from distinct charge and magnetic scattering mechanisms. This different spectral dependence evident in Fig. 2 is more completely revealed in energy scans at fixed q. Figure 3 shows data collected at the low and high q peaks across the L_3 line revealing that systematic differences persist across the entire energy range.

Modeling of these scattering spectra requires knowledge of the Co resonant magnetic and charge scattering factors, as well as values for f_{Pt}, f_{Cr}, and possibly other elements that may contribute to scattering contrast (*e.g.*, buffer or capping layers). The real and imaginary parts of these scattering factors are plotted in Fig. 4 (a) and (b), respectively. Resonant data for Co are obtained from measurements as described above, while non-resonant data for Pt and Cr are obtained from tabulated values [17]. The charge scattering factors for Co are determined from $f_c = (f_+ + f_-)/2$ and are non-zero everywhere except where Re[f_c] crosses zero, while the magnetic part $f_m = (f_+ - f_-)/2$ is zero everywhere except near the 2p levels. The slowly varying but significant scattering power of Pt and Cr can make important contributions to the spectral shapes, as seen below. While Im[f] accounts for photoelectric absorption, it also contributes to scattering together with Re[f].

It is useful to calculate (perhaps) oversimplified resonant scattering spectra to gain some insight into how different spectral shapes can arise. Spectra from several very simple contrast models are shown in Fig. 5, and the models briefly described here. Figure 5a shows the spectrum for the simplest model of pure magnetic contrast. This model assumes scattering from regions of oppositely oriented Co magnetization, in which scattering contrast is simply given by $a_m = f_+ - f_- = 2f_m$, or by the difference in Co scattering factors for opposite helicity circular polarization [11]. The scattered intensity is $4f_m^* f_m$, and exhibits two unipolar peaks. Figure 5b shows the spectrum for Co charge scattering contrasted with vacuum, while Fig. 5c shows the spectrum for Co charge scattering contrasted with Cr charge scattering.

Both of these spectra have resonant peaks showing more bi-polar character, and with different symmetry from each other. Figure 5d shows the spectrum for just the magnetic part of the Co scattering contrasted with Cr charge scattering. These model spectra demonstrate how very different spectral shapes can result from contrast models involving the difference between charge and magnetic resonant Co features and regions defined by other scattering amplitudes.

More realistic spectral modeling proceeds by positing a physically plausible scattering contrast model, calculating the scattering spectra predicted by that model, comparing with measured spectra, and iterating with changes to the model until reasonable agreement between model and data are obtained. Model spectra are multiplied by the measured transmission spectrum (for linearly polarized radiation) because the measured spectrum is also attenuated in this way.

The scattering spectrum at the low q peak is considered first. Hypothesizing, as above, that this scattering is predominantly magnetic in origin, it is appropriate to assume the pure magnetic scattering model in Fig. 5a. While the scattering power of the individual domains contains contributions from resonant Co charge and magnetic as well as non-resonant components from other constituents, the scattering contrast between domains remains $2 f_m$ and the intensity spectrum given by $4 f_m^* f_m$. If the magnetization of adjacent domains is not strictly antiparallel this intensity will simply be reduced by a constant, and so this simple model applies to these media films having a random distribution of in-plane magnetization. This intensity spectrum is plotted together with a small non-resonant (charge) background after scaling to the measured spectrum as the solid line in Fig. 3. The good agreement between this simplest model and measured spectra parallels a similar finding for scattering from magnetic domains in Co/Pt multilayers in ref. 11. In both cases it is seen that pure magnetic scattering, as defined above, exhibits characteristic peaks at the L_3 and L_2 white lines. The close agreement between model and measured spectra is a clear indication that the peak at lower q results predominantly from interference between regions of differently oriented magnetization separated by ~ 50 nm.

A different model is used to model the energy spectrum of the of the higher q peak. Its different spectral shape compared to the lower q peak, and the close correspondence of its position to the polycrystalline grain size, suggests investigation of models involving chemical scattering between Co-rich regions (presumably ferromagnetic) and Co-deficient regions (presumably paramagnetic). While many such models exist that would be consistent with the overall nominal composition, a simple model is considered here that provides a reasonable fit to the data. This model is based on the notion that segregation of Cr to grain boundaries yields a polycrystalline structure in which grain centers are Co-rich and ferromagnetic, while grain boundaries are Co-deficient and paramagnetic, on average. To simplify the model further, we assume that the Pt is entirely distributed in the Co-rich ferromagnetic phase. With these assumptions, specifying the relative scattering density of the Co-rich and Co-deficient phases as a linear combination of scattering factors then determines the model's scattering spectrum. The dashed line in Fig. 3 is a scaled model calculation assuming the Co:Pt:Cr ratio in the Co-rich phase to be 20:2:1, and the Co:Cr ratio in the Co-deficient phase to be 1:1. The same number density is assumed for each phase, and the scattering amplitude is calculated from $a_{ch\arg e} = a_A - a_B$ where $a_{A,B}$ are the scattering amplitudes of each phase given by the appropriate linear combination of charge scattering factors f_{Co}, f_{Pt} and f_{Cr}. This model spectrum quite reasonably approximates the measured higher q spectrum, and together the two model spectra capture the essential differences between the two measured spectra.

While it is not claimed that either of these two models is unique or provides a best fit to the measured spectra, experience calculating a variety of different model spectra does suggest that resonant magnetic and charge scattering are predominantly responsible for the low and high q peaks, respectively. This in turn supports the general picture of the microstructure of CoPtCr longitudinal recording media in which chemical segregation to grain boundaries is somewhat effective in reducing magnetic correlation lengths. Significant new information available from the resonant SAS is that quantitative measures of the enxemble-averaged magnetic and chemical grain size can be determined and that magnetic correlation lengths remain much larger than the polycrystalline grain size. This suggests either that intergrain

9

exchange interactions remain relatively strong or that the in-plane texture of the c axis, while random on average, may not be entirely random at the intergranular level.

Refinements to this spectral modeling approach may lead to better agreement with measurements and provide a more realistic picture of the segregation processes leading to heterogeneous magnetic and chemical microstructure. For example, we expect a magnetic-charge interference term in addition to the pure charge term used to model the high q peak in Fig. 3, since our model assumes both magnetic and chemical heterogeneity at this length scale. Indeed the magnetic-charge scattering model in Fig. 5d suggests that addition of this (or a similar) cross-term to a charge-charge term is consistent with, and may improve, the agreement of the model and measured spectra. Consideration of physical constraints including conservation of mass during segregation and the density and volume fraction of different phases will further refine modeling. While many parameters are needed to completely specify explicit SAS models involving segregation in a ternary system and both magnetic and charge scattering, it should be possible to simplify such models sufficiently so that traditional fitting procedures will yield experimentally derived values (or bounds) for the nominal compositions and volume fractions of segregated chemical and magnetic phases.

4. Conclusions

In summary, the CoPtCr film studied here is the second system from which we have resolved resonant scattering from magnetic length scales distinctly longer than chemical length scales based on the different spectral characteristics of resonant magnetic and charge scattering. This case demonstrates that scattering from magnetic heterogeneity in films having in-plane anisotropy is easily measurable, albeit reduced compared to the chemical scattering in the traditional transmission SAS geometry used. Modeling of the scattering spectra using measured resonant scattering factors is emerging as an effective and general means to separate charge from magnetic scattering. It appears that systematic variation of model parameters will enable bounds to be placed on chemical compositions responsible for scattering contrast between different phases, thereby providing information on nanoscale chemical segregation

10

difficult to obtain otherwise. The strong resonant scattering from both magnetic and chemical structure makes these scattering and spectral modeling techniques generally applicable to a broad range of magnetic (and other) films, and other nanostructured and heterogeneous bulk materials.

References

1. J. B. Kortright, D. D. Aswchalom, J. Stöhr, S. D. Bader, Y. U. Izderda, S. S. P. Parkin, I. K. Schuller, H.-C. Siegmann, J. Magn. Magn. Mat. 207 (1999) 7.

2. J. B. Kortright, Sang-Koog Kim, Phys. Rev. B 62 (2000) 12216.

3. O. Hellwig, J. B. Kortright, K. Takano, E. E. Fullerton, Phys. Rev. B 62 (2000) 11694.

4. J. B. Kortright, S.-K. Kim, E. E. Fullerton, J. S. Jiang, S. D. Bader, Nucl. Instrum. Methods A (in press).

5. Sang-Koog Kim, J.B. Kortright, Phys. Rev. Lett. 86, (2001) 1347.

6. J. B. Kortright, J. Appl. Phys. 70 (1991) 3620.

7. J. F. MacKay, C. Teichert, D. E. Savage, M. G. Lagally, Phys. Rev. Lett. 77 (1996) 3925.

8. J. W. Freeland, K. Bussmann, Y. U. Idzerda, C.-C. Kao, Phys. Rev. B. 60 (1999) R9923.

9. H. A. Dürr, E. Dudzik, S. S. Shesi, J. B. Goedkoop, B. van der Laan, M. Belakhovsky, C. Mocuta, A. Marty, Y. Samson, Science 284 (1999) 2166.

10. B. Hu, P. Geissbuhler, L. Sorensen, S. D. Kevan, J. B. Kortright, E. E. Fullerton, Synchrotron Radiation News 14 (2001) 11.

11. J. B. Kortright, S.-K. Kim, G. P. Denbeaux, G. Zeltzer, K. Takano, E. E. Fullerton, Phys. Rev. B 64 (2001) 092401.

12. S. K. Sinha, E. B. Sirota, S. Garoff, H. B. Stanley, Phys. Rev. B 38 (1988) 2297.

13. R. M. Osgood III, S. K. Sinha, J. W. Freeland, Y. U. Idzerda, S. D. Bader, J. Magn. Magn. Mater. 198 (1999) 698.

14. D. Weller and A. Moser, IEEE Trans. Magn. 35 (1999) 4423.

15. M. F. Doerner, K. Tang, T. Arnoldussen, H. Zeng, M. F. Toney, D. Weller, IEEE Trans. Magn. 36 (2000) 43.

16. L. Li, M. Mirzamaani, X. Bian, M. Doerner, S. Duan, K. Tang, M. F. Toney, T. Arnoldussen, and M. Madison, J. Appl. Phys. 85 (1999) 4286.

17. B. L. Henke, E. M. Gullikson, J. C. Davis, At. Data Nucl. Data Tables 54 (1993) 181; and at http:/www-cxro.lbl.gov/optical_constants/.

Figure Captions

Figure 1. The symmetric transmission scattering geometry used here optimizes coupling of the scattering vector **q** (defined by incident and scattered wavevectors $\mathbf{k_o}$ and $\mathbf{k_f}$) to both magnetic and chemical structure in the film plane. Scattering from magnetic domains with magnetization in two limiting orientations is considered: (a) perpendicular anisotropy, and (b) in-plane anisotropy. Ferromagnetic domains are shaded with magnetization vectors as indicated. Chemical structure is not depicted.

Figure 2. Scattered intensity vs. q measured from a CoPtCr alloy taken at different energies as noted across the Co L_3 white line. Two peaks are apparent, indicating interference between features having two distinct length scales. Using $2\pi/q$ to estimate the length scales gives 48 nm and 11 nm for the lower and higher q peaks, respectively. Note the different energy dependence of the two peaks.

Figure 3. Scattering spectra (symbols) measured at the two distinct peaks in reciprocal space, as noted. Spectra calculations (lines) based on measured resonant Co scattering factors and specific models as described in the text.

Figure 4. Measured resonant atomic scattering factors for Co are plotted across its L_3 and L_2 lines at 779 and 794 eV, respectively. Tabulated data for Pt and Cr are also displayed. The real part of the scattering factors are plotted in (a), and the imaginary part in (b). While the imaginary part of the scattering factor describes photoelectric absorption, it also contributes to scattering.

Figure 5. Simulated resonant scattering spectra for very simple models as indicated (see text for details).
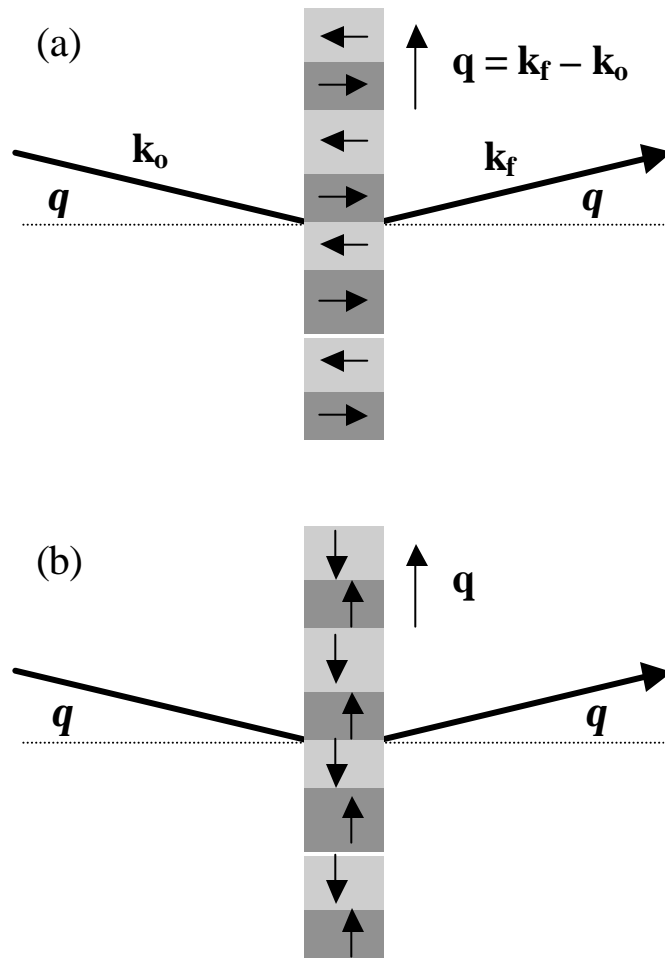
(a)

$\mathbf{q} = \mathbf{k_f} - \mathbf{k_o}$

$\mathbf{k_o}$

$\mathbf{k_f}$

q

q

(b)

$\mathbf{q}$

q

q

Figure 1

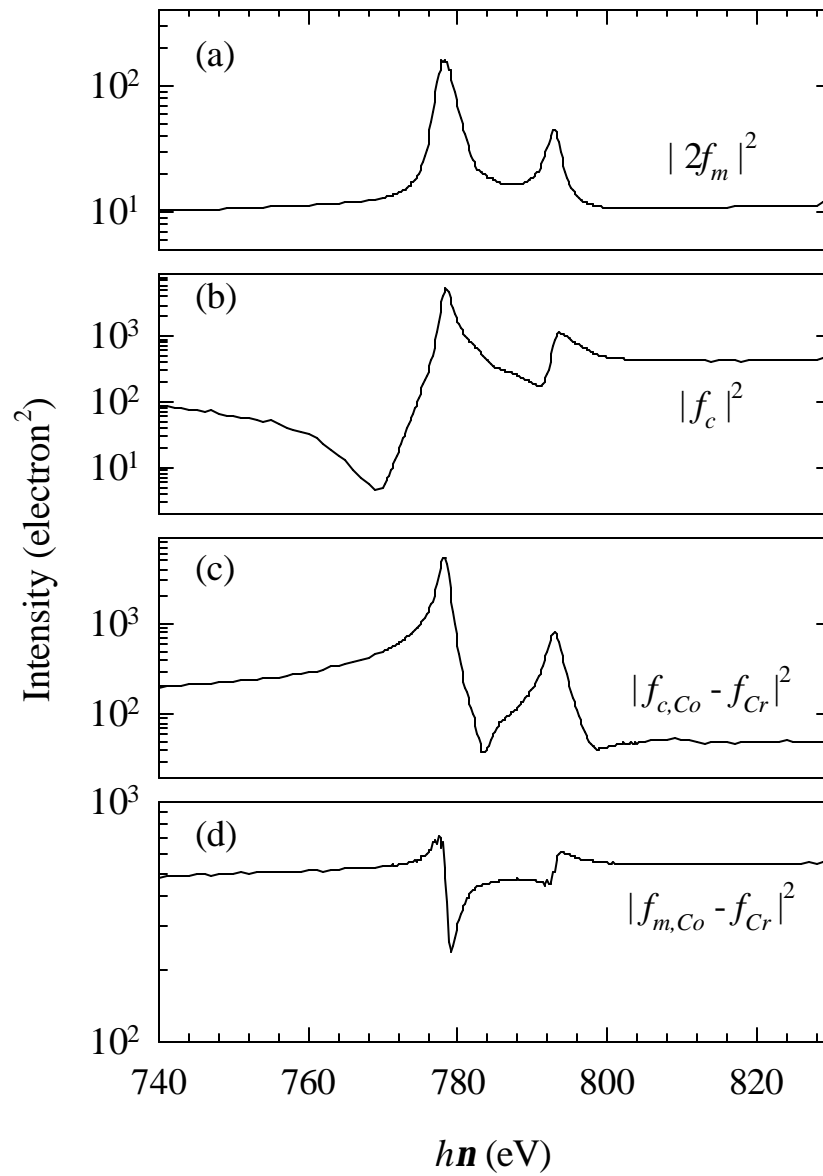Kortright, *et al.*, Figure 1
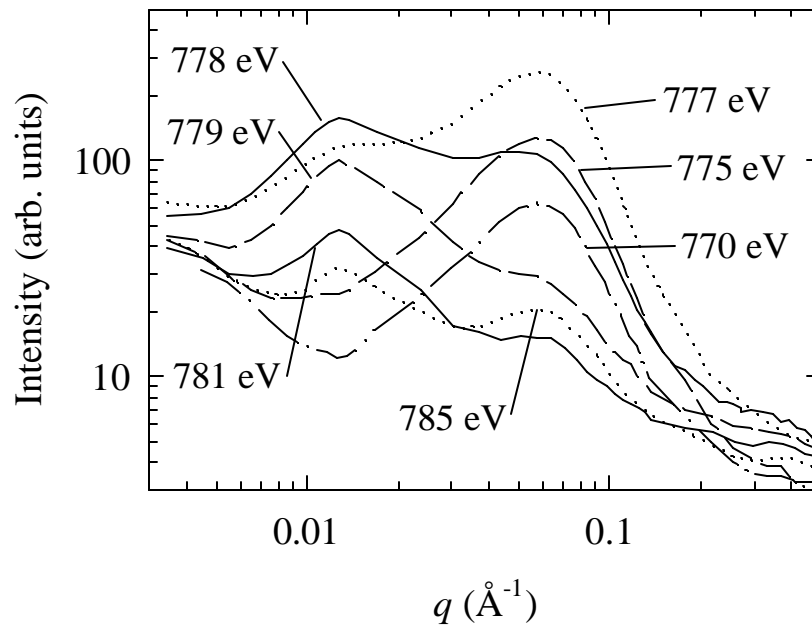
Figure 2
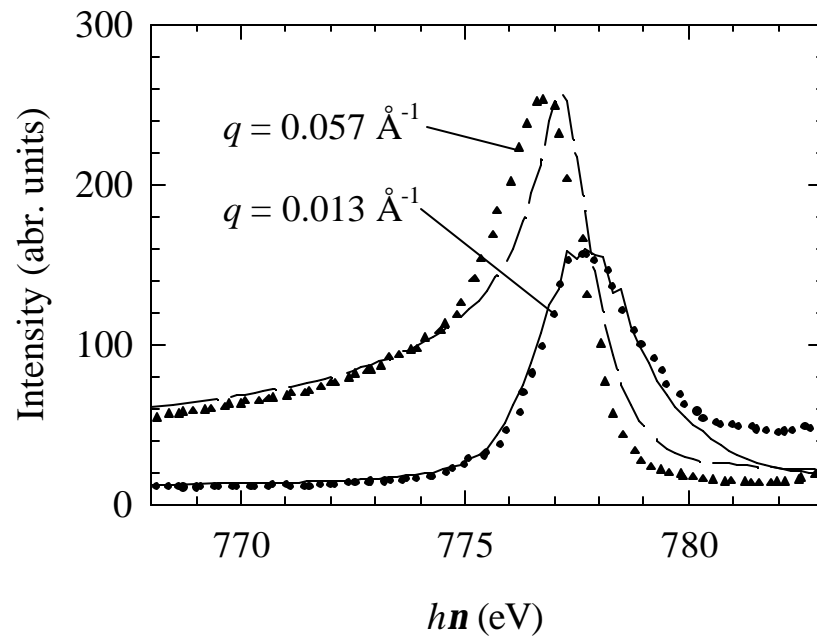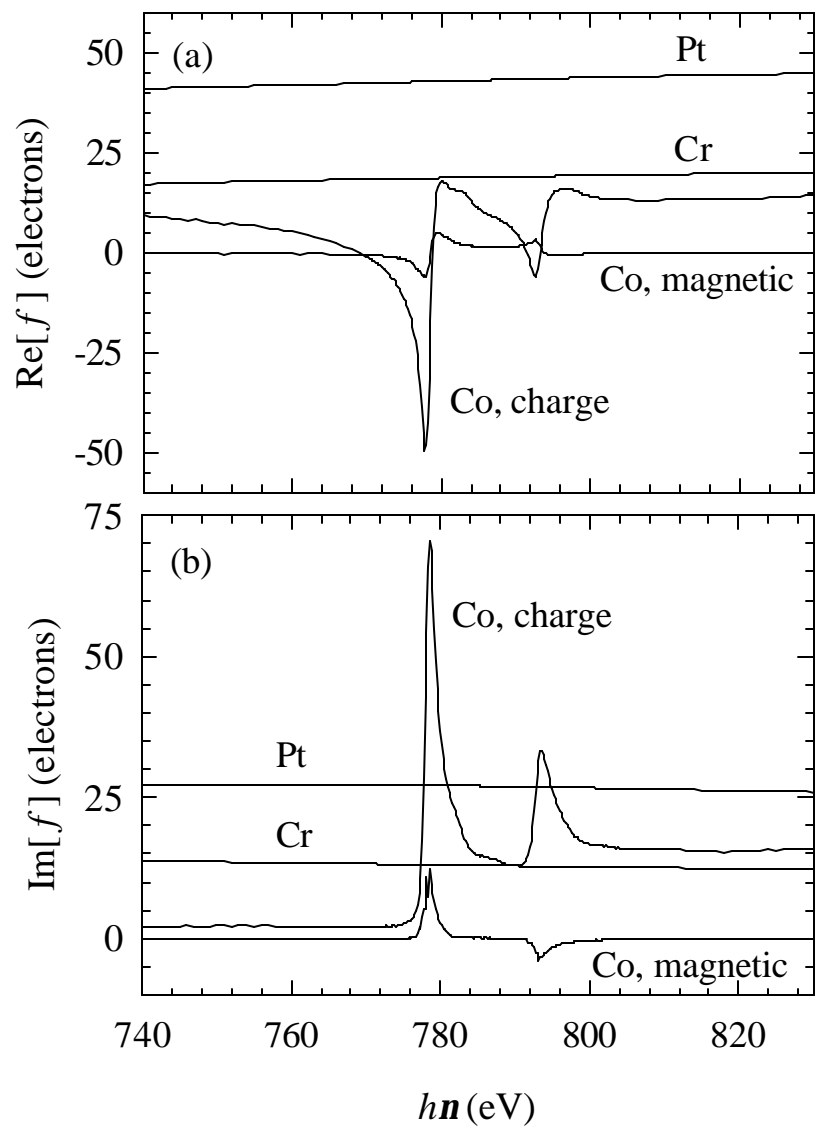
Figure 3

Figure 4

Figure 5

Kortright, *et al.*, Figure 5